

## Excitation of low-lying excited states of hydrogen in 1–5-keV collisions of $H^-$ with He, Ar, Xe, and $N_2$ †

M. Harnois,\* R. A. Falk, R. Geballe, and J. Risley‡

Department of Physics, University of Washington, Seattle, Washington 98195

(Received 7 March 1977)

Cross sections for the production of excited hydrogen in the  $3d$ ,  $3s$ ,  $4s$ , and  $5s$  states have been measured for 1- to 5-keV  $H^-$  ions incident upon He, Ar, Xe, and  $N_2$ . The results show nominally flat cross sections which scale as a function of principal quantum number faster than  $n^{-3}$ . Comparison is made with similar results for  $np$  states, and the implication that these results may have on some recently proposed collision models is discussed.

### I. INTRODUCTION

This paper reports on the measurement of cross sections for detachment of  $H^-$  ions of energy 1–5 keV into various low-lying excited states of hydrogen resulting from collisions of  $H^-$  with rare-gas atoms and molecular nitrogen. These measurements were made by observing Balmer emission in the decay of the excited state of interest, and serve to complement similar measurements made in the Lyman series.<sup>1,2</sup>

Electron detachment dominates the total inelastic cross section for  $H^-$ . Until recently no measurements were reported of cross sections to individual states of the resulting hydrogen atom. Orbeli and co-workers measured cross sections for production of  $H(2p)$  and  $H(2s)$  over a range of  $H^-$  impact energy from 5 to 40 keV.<sup>1</sup> These measurements were made by monitoring Lyman- $\alpha$  radiation, in the case of  $H(2s)$  produced by electric field quenching of the metastable  $H(2s)$ .

Recently Risley and co-workers have extended the Lyman- $\alpha$  measurements to 1-keV incident  $H^-$  energy, and have also measured emission of Lyman  $\beta$ , Lyman  $\gamma$ , and Lyman  $\delta$ .<sup>2</sup> These measurements result in cross sections for excitation of  $H(2p)$ ,  $H(2s)$ , and  $H(3p)$ . In addition, results were presented for excitation of some mixed states produced by the small electric fields encountered in their apparatus.

Because dipole selection rules favor the detection of the  $np$  series of states in the Lyman series, the current series of measurements of Balmer radiation was made to determine cross sections for the  $ns$  and  $nd$  states. These measurements then serve to complement the  $np$ -state measurements of Risley *et al.*

Since the negative hydrogen ion is a relatively simple two-electron system, it serves as a useful prototype for negative-ion detachment reactions. Information on apportionment of the total detachment cross section among individual ground-state

and excited-state hydrogen-atom output channels yields information about the dynamics of negative-ion detachment.

### II. METHOD

We wish to measure cross sections for the excitation of  $H(ns)$  and  $H(nd)$  from Balmer emission. The very small fine-structure separation in hydrogen precludes optical resolution of the radiation from states of different angular momentum, but to separate their contributions we can exploit the fact that different angular momentum states decay with significantly different lifetimes. Because the negative hydrogen ion loses little momentum in stripping collisions with the target atom, the residual excited hydrogen atom travels with nearly the primary beam velocity in the laboratory system. Atomic states with different lifetimes will have different and characteristic spatial distributions of radiation.

The study of such distributions has a long history<sup>3</sup> and enjoyed a renaissance with the study of radiation emanating from a fast beam of particles in collision with a foil target.<sup>4</sup> These techniques were first applied to cross-section measurements from thin gas targets by Hughes and co-workers.<sup>5</sup> Hughes *et al.* have measured cross sections for the production of low-lying excited states of hydrogen in collisions of protons and neutral hydrogen atoms with gas targets using a technique similar to that reported here.

In order to predict the spatial distribution of radiation from an excited state in the beam, consider the density of an excited state  $j$ ,  $n_j$ , as a function of the distance  $y$  from the target entrance. This density is governed by the differential equation

$$dn_j/dy = -n_j(1/v\tau_j - \sigma_{ji}n_i) + n_i n_i \sigma_j + \sum_{i>j} n_i (A_{ij}/v). \quad (1)$$

The beam velocity is  $v$ ;  $n_b$  and  $n_t$  are the beam and target densities, respectively;  $\tau_j$  is the natural lifetime of the  $j$ th excited state;  $A_{ij}$  is the spontaneous transition probability from state  $i$  to state  $j$ ;  $\sigma_{jt}$  is the total loss cross section for the excited state  $j$  in collisions with the target;  $\sigma_j$  is the production cross section for the state  $j$  in collisions with the target; and  $n_i$  are excited-state densities for states of higher excitation.

The first term describes the decline in excited-state population due to natural decay and collisional deexcitation. The second term describes the production of the excited state as a consequence of collisions with the target atom. The last sum accounts for cascade population of the excited state from states of higher excitation. Because of the last term, and the fact that similar equations govern the densities  $n_i$ , the system to be solved is a coupled set of differential equations. If we neglect this cascade contribution for the moment, Eq. (1) can be solved, and predicts an exponentially growing population of excited states in the beam as it traverses the target region. We have provision to pass the beam through the target and into an evacuated flight region. Once the beam has left the target region,  $n_t = 0$  and in the absence of cascade, Eq. (1) becomes

$$\frac{dn_j}{dy} = -n_j \frac{1}{v\tau_j}, \quad (2)$$

and simple exponential decay results.

Because of the large detachment cross section for the  $H^-$  beam, there is an increasingly significant component of neutral hydrogen in the beam as it traverses the target region. The fraction of protons remains insignificant. The second term in Eq. (1) containing the beam density, and excitation cross section should therefore be rewritten as a sum of two terms:

$$n_{b0}n_t\sigma_{j0} + n_{b-}n_t\sigma_{j-}, \quad (3)$$

where the additional subscript affixed to the density refers in the conventional manner to the charge state of the beam. Expressions for  $n_{b0}$  and  $n_{b-}$  are given by well-known relations in terms of known attachment and detachment cross sections.<sup>6</sup>

Including the above complication and neglecting for the moment the sum that represents cascade, Eq. (1), as modified by Eq. (3), can be solved exactly:

$$n_j(y) = n_{b-}(0)n_t y_j (\sigma_{j-} F_{j-} + \sigma_{j0} F_{j0}). \quad (4)$$

Here  $n_{b-}(0)$  is the  $H^-$  beam density at the target entrance ( $y=0$ ), and  $y_j$  is a characteristic length equal to the product of the beam velocity and the natural lifetime  $\tau_j$ . The coefficients  $F_{j-}$  and  $F_{j0}$

are given by

$$F_{j-}(y) = \frac{\sigma_{0-1}}{\sigma_{tot}} \frac{[1 - \exp(-y/y_j - n_t y \sigma_{jt})]}{1 + n_t y_j \sigma_{jt}} + \frac{\sigma_{-10}}{\sigma_{tot}} \frac{[\exp(-n_t y \sigma_{tot}) - \exp(-y/y_j - n_t y \sigma_{jt})]}{1 + n_t y_j \sigma_{jt} - n_t y_j \sigma_{tot}} \quad (5)$$

and

$$F_{j0}(y) = \frac{\sigma_{-10}}{\sigma_{tot}} \frac{[1 - \exp(-y/y_j - n_t y \sigma_{jt})]}{1 + n_t y_j \sigma_{jt}} - \frac{\sigma_{-10}}{\sigma_{tot}} \frac{[\exp(-n_t y \sigma_{tot}) - \exp(-y/y_j - n_t y \sigma_{jt})]}{1 + n_t y_j \sigma_{jt} - n_t y_j \sigma_{tot}}. \quad (6)$$

The symbols  $\sigma_{-10}$  and  $\sigma_{0-1}$  refer to the detachment and attachment cross sections, respectively, and  $\sigma_{tot}$  is the sum of the two.

We are able to observe the excited-state decay both inside the target region,  $0 \leq y \leq L$ , and in an evacuated decay region,  $y > L$ . The solution given by Eqs. (4)–(6) applies inside the target region. The solution to Eq. (2) in the decay region is simply

$$n_j(y) = n_j(L) \exp[-(y-L)/y_j]. \quad (7)$$

For the purposes of the next paragraphs we can allow the exponential term in Eq. (7) to be absorbed in the definition of  $F_j$ . For  $y \leq L$ ,  $F_j$  is now defined by Eqs. (5) and (6). For  $y > L$ ,  $F_j$  is given by

$$F_{j-}(y) = F_{j-}(L) \exp[-(y-L)/y_j] \quad (8)$$

and

$$F_{j0}(y) = F_{j0}(L) \exp[-(y-L)/y_j]. \quad (9)$$

The Balmer signal can be written

$$\dot{N} = \frac{Vd\Omega}{4\pi} \epsilon \sum_j n_j A_{j2}, \quad (10)$$

where  $Vd\Omega/4\pi$  is the effective-volume-solid-angle product for the detector,  $\epsilon$  is the detection efficiency, and  $A_{j2}$  is the transition probability from the state  $j$  to the dipole allowed state with principal quantum number 2. Using our result for  $n_j$  we can write for the Balmer signal as a function of  $y$ ,

$$\dot{N}(y) = I_0 n_t \frac{Vd\Omega}{4\pi} \epsilon \sum_j \gamma_j [F_{j-}(y)\sigma_{j-} + F_{j0}(y)\sigma_{j0}] \quad (11)$$

where  $I_0$  is the number of ions/sec, the effective-volume-solid-angle product has become an effective-length-solid-angle product, and  $\gamma_j$  is the branching ratio for the state  $j$  in the Balmer series, where

$$\gamma_j = A_{j_2} \tau_j = A_{j_2} y_j / v. \quad (12)$$

Equation (11) gives the detected signal in terms of the incident beam intensity, the target density, the natural lifetime of the excited states, and several cross sections including the excitation cross section,  $\sigma_{j-}$  we wish to measure. Values for the cross sections  $\sigma_{j_0}$  have not been measured in this energy regime. We therefore choose target densities such that  $F_{j-} \gg F_{j_0}$ . The derived values for  $\sigma_{j-}$  are not significantly altered for a wide range of assumed values for  $\sigma_{j_0}$ . As we use narrow bandpass filters, the sum over states contains only terms referring to states with the same principal quantum number and differing angular momentum.

### III. STARK MIXING

The foregoing analysis depends upon our ability to calculate and utilize the proper natural lifetimes for the set of fine-structure states corresponding to a given principal quantum number. Because the fine structure for hydrogen is small, electric fields of less than 1 V/cm require a new set of diagonal states which may be significantly perturbed from the field-free basis of  $nl$  states.<sup>7</sup> The new states made up of linear combination of  $nl$  states have new and different lifetimes and branching ratios in the Balmer series. The field-free states are said to be "Stark mixed" by the perturbing electric field.

In our experiment there are three possible sources of such electric fields. They can arise if surfaces which view the beam are not equipotential, from space charge from the beam itself, and from the motion of the charged particle in the magnetic field of the laboratory. Fields due to this last cause, which are estimated to be 0.4 V/cm for a 5 keV beam particle, will dominate all others for beam velocities corresponding to 1 keV ion energies and greater. These fields complicate the analysis and prevent the measurement of  $4d$  and  $5d$  cross sections due to the mixing of the  $j \geq \frac{3}{2}$  magnetic substates with those of the  $p$  and  $f$  states.

### IV. PROCEDURES

The spatial distribution of radiation was measured using an apparatus of conventional nature as shown in Fig. 1. The transparent flight tube is glass process pipe which has been coated on the interior with a thin layer of conductive tin oxide. A movable photometer is able to view both the build-up region between the two target bulkheads, and the decay region between the second target bulkhead and the Faraday cup. The differential

pumping ratio between the target and the decay region is approximately 60. Since this ratio leads to a finite pressure in the decay region, the Balmer signal in this region must be corrected for beam-background-gas collisions. This correction is accomplished by making provision to admit gas into the decay region while evacuating the target region. During these measurements the pressure in the decay region, as monitored by the ionization gauge near the Faraday cup, is made equal to that observed during signal-taking. The background signal so obtained is then subtracted from the signal measured with gas admitted through the target region. A capacitance manometer monitors the target-region pressure. Commercial, "ultra pure" grade gases were used.

The photometer collects light with an  $f/1$  lens from a section of beam of length 0.5 to 2 cm, controlled by a field stop. The light is collimated and passed at normal incidence through interference filters of approximately 7.5 nm full width at half maximum (FWHM). Even at  $f/1$  collection angles, Doppler frequency shifts are not important at energies below 5 keV. For Balmer- $\alpha$  radiation an S-20 photomultiplier was used, but for Balmer- $\beta$ , and Balmer- $\gamma$  measurements a Bialkali photomultiplier was substituted. The S-20 tube was cooled to approximately  $-10^\circ\text{C}$  to lower its dark rate, while the Bialkali tube was run at room temperature. The output of both tubes was single-photon-counted at each photometer position for the amount of time necessary to integrate the Faraday cup current to a preset amount of charge.

Since this series of measurements was normalized to other cross-section measurements,<sup>8</sup> no attempt was made to determine values for the efficiency or length-solid-angle product. As re-

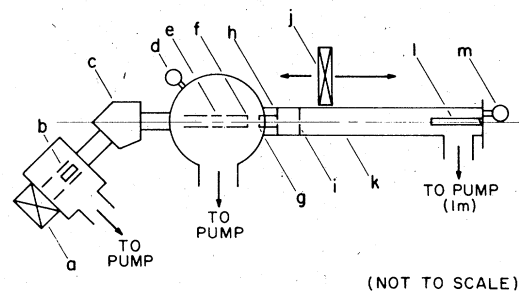


FIG. 1. Schematic drawing of the apparatus. (a) Duo-plasmatron source; (b) einzel and quadrupole lenses; (c) mass analysis magnet; (d) ionization gauge; (e) einzel lens; (f) first beam collimator; (g) second beam collimator; (h) first target bulkhead and aperture; (i) second target bulkhead and aperture; (j) movable photometer; (k) transparent flight tube; (l) Faraday cup; (m) ionization gauge.

quired by Eq. (6), we measured the time integral of  $\dot{N}(y)$  and  $I_0$ , and monitored target density,  $n_t$ . The branching ratios,  $\gamma_j$ , are known, and the functions  $F_{j-}(y)$  and  $F_{j_0}(y)$  are calculable from known cross sections. In our situation the target was quite thin and  $F_{j-} \gg F_{j_0}$  so that we may correct for the neutrals adequately by a reasonable estimate for  $\sigma_{j_0}$ . We analyze our data with the assumption of equal cross sections for H and  $H^-$  impact. Measurements were taken for many values of  $y$ . Each measurement was taken for the same integrated current after corrections for detachment losses and was normalized to a common value for target density.

The ensemble of signal versus distance determinations showing the effect of the background gas is given in Fig. 2. The target length was 10 cm though some data were taken with other lengths. The absence of data in the region of 10 cm is due to a "blind spot" caused by the target bulkhead.

Several phenomena may affect the cross-section measurements in addition to those already mentioned. First, contributions to the state population arising from cascade transitions have not been included in Eq. (2). An estimate of the magnitude of this effect was made as follows. Several low-lying cross sections of interest have been measured in this experiment and the work of Risley *et al.*<sup>2</sup> These results point to  $p$ -state cross sections that scale with principal quantum number  $n$  approximately as  $n^{-3}$ , and  $s$ -state cross sections that scale as  $n^{-4}$ , see Fig. 5. As a worst-case approximation, a model calculation was performed which assumed  $n^{-3}$  scaling and assessed the contribution to the measured Balmer- $\beta$  radiation by cascade from  $n=5$  and  $n=6$  populations via the system of equations represented by Eq. (1). The results are shown for assumed field free states in Fig. 3. The results show little distortion of the shape of the decay curve, but produce a 12% correction to the extracted  $p$ - and  $d$ -state cross

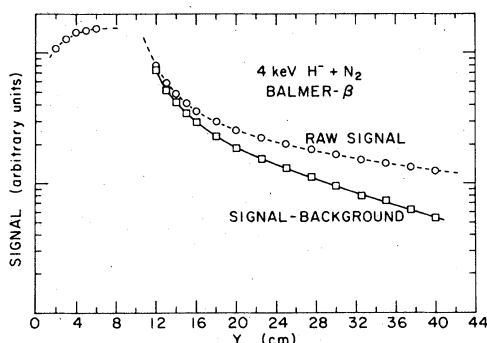


FIG. 2. Sample data illustrating effect of finite decay region pressure: circle, raw signal; square, signal with background subtracted.

sections, and a small effect on the derived  $s$ -state cross section. Second order, or double cascade, which would be expected to alter the long-lived  $s$  states the most are not incorporated in this model, but we always reproduce the  $s$ -state lifetimes correctly, and so have no reason to suspect that second-order processes are significant. It should be emphasized that since the experimental evidence indicates scaling closer to  $n^{-4}$ , cascade corrections should be less than a few percent. No cascade corrections have been applied to any of the data presented here.

In reporting measurements of total cross sections from emission data taken over a restricted solid angle, proper allowance must be made for the possible anisotropy of emission due to polarization.<sup>9</sup> Of the cross-section measurements reported here, only the  $3d$  cross section is subject to such effects. The polarization fraction of  $3d$  emission was measured for all gases by measuring the intensity parallel and perpendicular to the beam line through HN-38 Polaroid material. The measured polarization fraction for the total emission declined steadily as a function of  $y$ . The maximum observed value was less than 0.10 for any gas, and corresponding inferred values for the  $3d$  polarization fraction were less than 0.30 for the most reliable data. Corrections to our total cross sections would therefore be at most 10%. However, measurements of the polarization fraction were not demonstrated to be independent of distance as they should be. Because of our inability to bound the values of the derived  $3d$  polarization as the fraction of  $3d$  radiation declined to zero, no corrections have been applied to the  $3d$  cross-section values reported here.

The second term in Eq. (1) accounts for depopulation of the excited state via collisions with the target gas. The cross sections for such processes are in general not known for our work, but related cross sections have been measured,<sup>10</sup> and they may

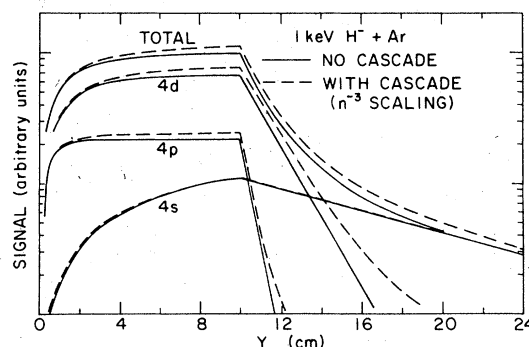


FIG. 3. Results of model calculation for first-order cascade with assumed  $n^{-3}$  scaling and field free  $n=4$  states.

be expected to be large. Corrections have not been applied because of the uncertainty about the size of the relevant cross sections.

All cross sections presented here are based upon measurements taken at target pressures less than 0.25 mTorr where we observe no deviation from linearity with changing target pressure. The cross sections we report are derived from fits where the effect of  $\sigma_{j+}$  has been effectively neglected by using very small values for  $\sigma_{j+}$ . If we fit our data to Eq. (11) with an assumed value of  $2 \times 10^{-15}$  cm<sup>2</sup> for all  $\sigma_{j+}$ , the results for  $\sigma_{j-}$  differ from those reported by less than 7%.

## V. MEASUREMENTS

### A. $n=3$ cross sections

In this series of measurements the Earth's field barely mixes the  $3P_{3/2}$  ( $m = \frac{3}{2}$ ) state with the  $3D_{3/2}$  ( $m = \frac{3}{2}$ ). The mixing results in a shift of less than 2% in either lifetime, and hence is unobservable in our apparatus. We analyze our data on the basis of field-free states.

The cross section for production of  $3p$  excited states is small enough that, in conjunction with the small branching ratio in the Balmer, the  $3p$  signal is too small in the target region to enable reliable values for  $3p$  production cross sections to be found. In addition there is little data outside the target region since the  $3p$  decay length is quite small over our energy range. However, at the higher energies, for He and Ar targets we can do a least-squares fit to the entire light curve to find  $3p$  cross sections that agree within  $\pm 40\%$  with the values obtained from the stronger Lyman emission.<sup>2</sup> We may derive  $3s$  and  $3d$  cross sections by (1) performing a least-square fit to the light curve as a whole; (2) performing a least-square fit to only the data at large  $y$  where there is no  $3p$  or  $3d$  contribution, thus obtaining the  $3s$  cross section, and then, using this value, determine the  $3d$  cross section from the rest of the decay curve; or (3) obtaining a value for the  $3s$  cross section from (1) or (2), and utilizing the  $3p$  values from Ref. 2, determine the  $3d$  cross section from the target region emission. For He and Ar where data are available from Ref. 2, all three methods agree within 10% except for the case of 1- and 2-keV  $3d$  cross sections where methods (1) and (2) yield abnormally large  $3d$  cross sections and correspondingly extremely small  $3p$  cross sections. At these energies little information is available for the  $3d$  decay since, for example, at 1 keV the  $3d$  decay length is about 0.7 cm. Therefore it is concluded that method (3) gives the most reliable results and it is adopted at 1 and 2 keV.

For Xe and N<sub>2</sub> no accurate  $3p$  results exist, and hence we use only methods (1) and (2) for energies of 2 keV or greater. However, reliable  $3d$  data at 1 keV are not obtainable in this manner. We feel that we can reliably estimate the  $3p$  cross sections within a factor of 2 from the higher energy results, and *assume* relative energy independence of these cross sections to derive  $3d$  results from the target data as in method (3). Because of the small  $3p$  branching ratio, the uncertainty in this procedure is less than 10%. The results for the  $3d$  and  $3s$  cross sections are shown in Fig. 4.

The Balmer- $\alpha$  cross sections have been put on an absolute basis by measuring the emission of Balmer  $\alpha$  from the  $3s$  state arising from the collision of 5-keV H<sup>+</sup> with Ar. The cross section for this process at this energy has been measured by Dawson and Loyd as  $3.6 \times 10^{-18}$  cm<sup>2</sup>.<sup>3</sup> Measurements for proton impact can be made in the present apparatus with no significant change except for beam species. Consequently proton checks were made often during the course of the work. Values for  $(I d\Omega/4\pi)$  obtained from such measurements showed no systematic drifts and were subject to the same  $\pm 5\%$  reproducibility that characterized all the data.

The uncertainty in the measured cross sections due to possible systematic error is estimated to be  $\pm 20\%$  for these measurements. The cross section to which ours are normalized traces its absolute value to a spectrometer calibrated to  $\pm 40\%$ .<sup>11</sup>

### B. $n=4$ cross sections

For the case of Balmer- $\beta$  radiation, fields in the frame of the moving atom due to the magnetic

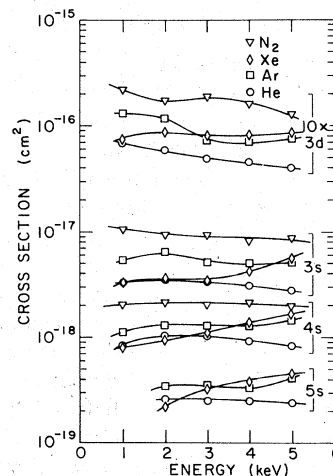


FIG. 4. Cross sections for excitation of H( $3d$ ), H( $3s$ ), H( $4s$ ), and H( $5s$ ) in collisions of H<sup>-</sup> with molecular nitrogen, xenon, argon, and helium. The results for H( $3d$ ) have been multiplied by 10.

field of the earth can cause significant mixing between states of different  $l$  for  $j = \frac{3}{2}$  and  $\frac{5}{2}$ . Probably only the  $4F_{5/2}$  state contributes significantly to radiation that would otherwise be ascribed to the  $4d$  level, and our results are generally consistent with a pure-state lifetime of 36 ns for the apparent  $4d$  radiation. Nevertheless, at the highest energies measured we are able to extract more than a 36-ns component, and we feel that there may be some admixture of  $4f$  radiation. (The  $4F_{7/2}$  states have no branching ratio in the Balmer, but the  $4F_{5/2}$  states for  $m_j \geq \frac{3}{2}$  have a branching ratio of 0.50 and an apparent lifetime of 49 ns.) Earlier preliminary reports of these results presented values for  $4d$  cross sections,<sup>12</sup> but we no longer believe that reproducibility of pure-state lifetimes is a sensitive indicator of state purity. The  $4S_{1/2}$  state is unmixed, and we confine our Balmer results to this state.

The results for the  $4s$  cross sections are presented in Fig. 4. These values are placed on an absolute basis by measuring the cross section for production of  $H(4s)$  in 5-keV collisions of protons with Ar. This cross section has been measured to be  $8.5 \times 10^{-19} \text{ cm}^2$ .<sup>8</sup> The uncertainties in these values are the same as for the Balmer- $\alpha$  results.

#### C. $n = 5$ cross sections

In our apparatus nearly all states of the  $n = 5$  level where  $j \geq \frac{3}{2}$  are completely mixed at all beam energies utilized. The measured distribution of Balmer- $\gamma$  radiation is consistent with the assumption of fully mixed lifetimes. In addition, since the fields required for mixing vary approximately as  $n^{-5}$ , a calculation shows a small admixture of  $5P_{1/2}$  population to the  $5S_{1/2}$  state. As a result we reduce our data with the assumption of a  $5s$ -state lifetime 12% shorter than the field-free value at 5 keV, and must make additional corrections to our derived cross sections to account for the fact that some radiation is actually contributed by the  $5p$  state, and that the branching ratio from the mixed state is no longer the field-free value. These corrections amount to about 15% at 5 keV.

The results for cross sections for excitation of  $H(5s)$  are given in Fig. 4. There are no analogous Balmer- $\gamma$  cross sections for normalization, as there were for Balmer  $\alpha$  and Balmer  $\beta$ . We rely on a calibrated source of spectral irradiance to intercalibrate the photometer efficiency between Balmer  $\beta$  and Balmer  $\gamma$ .<sup>13</sup> Based upon the manufacturer's stated accuracy, we believe this procedure is accurate to 10%. In addition, because for Balmer  $\gamma$  we take data over a relatively smaller fraction of the decay curve, and because fewer data were taken, the uncertainties in the  $5s$  cross sections are larger than those for the

others. It is estimated that the data from this experiment alone may be uncertain to  $\pm 25\%$ .

#### VI. SUMMARY

We have measured excitation cross sections for the  $3s$ ,  $4s$ ,  $5s$ , and  $3d$  states of hydrogen produced in low-energy collisions of  $H^-$  with rare gases and molecular nitrogen. One obvious feature is the relative energy independence of the results, even allowing for the restricted energy range sampled in this experiment. The cross sections are relatively flat with no strong evidence of threshold behavior except in the case of Xe. In this regard, the results are reminiscent of those for H impact and dissimilar to the case of  $H^+$  impact.<sup>14</sup>

Orbeli *et al.* noticed that, over their energy range (5–40 keV), the cross section for  $2s$  and  $2p$  production in the case of  $H^-$  impact is two and perhaps three or more times larger than the analogous cross section for H impact. Our results, for states of principal quantum number 3, 4, and 5, can not be directly compared with any analogous cross sections measured for neutral impact. At 5 keV comparisons with data for  $n = 3$  and  $n = 4$  excitation extrapolated from 10 keV would indicate  $H^-$  cross sections to be 1.5 to 4 times larger than those for neutral impact. Significantly, at 1 keV, for  $2p$  and  $2s$  excitation where data exist,<sup>15</sup> the ratio of  $H^-$  to H impact cross sections, which is still 1.5 to 2 at 5 keV, has declined to nearly unity.

Orbeli *et al.* argued that the efficiency of  $H^-$  in producing  $H(2p)$  or  $H(2s)$  might be explained by a model due to Drukarev which ascribed the large  $n = 2$  cross sections to the large overlap between the wave function of the outer electron in the incoming ground-state negative hydrogen ion and the excited-hydrogen wave function.<sup>16</sup> In this model the use of the Born approximation produces a cross section dominated by a mechanism requiring the detachment of the inner electron followed by a readjustment of the remaining electron to the new field, resulting in an abnormally large  $H(2s)$  excitation cross section.

For the higher values of  $n$  which are the subject of our work, the overlap will be small, so the Drukarev model would appear to fail to account for the large cross sections we find. However, the Born approximation, on which this model relies, is known to have dubious validity at the low energies used here. Consequently, our results are not necessarily at variance with the Drukarev model.

At the lowest energies used in this work, cross-section measurements for  $n = 2$  state production imply that the  $H^-$  impact collision looks very little different from neutral impact. The outer,

weakly bound electron may be stripped off at large internuclear distance, allowing the collision to proceed as a neutral-atom-rare-gas collision. At these low energies, there are no data for production of states of higher principal quantum number in collisions involving H impact. Therefore, we cannot test the application of this model to collisions studied in this work. At the highest beam energies used, the indication that the  $H^-$  impact cross sections are probably larger than those for H impact imply that the outer electron must be a participant.

Figure 5 compares the results of the present experiment with the  $np$  results of Risley *et al.* by plotting the log of the excitation cross sections versus the log of the principal quantum number. The ground-state cross sections have been synthesized from the total-detachment cross sections<sup>17</sup> by subtracting cross sections for excitation of the higher  $n$  levels. The " $np$ "-state results may contain some contribution from  $nD_{3/2}$  states at the higher  $n$  levels. The lines shown simply connect the points, and the scaling behavior indicated is provided only to assist in the reading of the graph.

Figure 5 indicates that the  $s$ - and  $p$ -state cross sections may scale somewhat differently. The "kink" in the  $p$ -state curve at  $n=2$  suggests a larger  $2p$  cross section than might be expected from scaling the higher  $np$  cross sections. If the collision were modeled as one involving early detachment of the outer electron at large internuclear distance, an examination of H-He or H-Ar molecular correlation diagrams might imply that the  $\sigma$ - $\pi$  rotational coupling between the incoming ground state and the  $2p$  excited state is contributing significantly.<sup>18</sup> However, as we have mentioned before, this model for the collision would seem to be in question at energies above 5 keV where the  $H^-$  impact cross sections are probably larger than those for H impact.

Rules for construction of a diabatic molecular correlation diagram for a negative-ion system

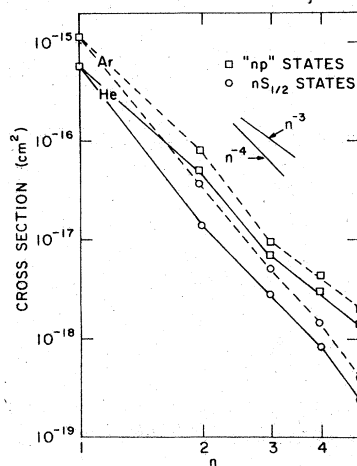


FIG. 5. Excited-state cross sections for 5 keV impact on He and Ar showing approximate scaling results. Ground-state cross sections are synthesized from the total detachment cross sections (Ref. 17) by subtracting the cross section to higher states. The  $ns$  cross sections are taken from this work and Ref. 1. The " $np$ " results are taken from Ref. 2. The highest  $np$  results may contain some contribution from  $nD_{3/2}$  levels.

are unclear. The identification of separated atom states is unambiguous, but for  $H^-$ -rare-gas systems, states that are the necessary limits for one-electron orbitals have not been shown to exist for times long with respect to the collision time.

Finally, it may also be pointed out that the ratio of  $3p$  to  $2p$  excitation, or the  $3s$  to  $2p$  ratio is not significantly different for  $H^-$ , H, or  $H^+$  impact at energies near 5 keV. The implication can be drawn that molecular promotion may affect the  $2p$  population, and "set the scale" for the various cross sections, but the apportionment of excited-state populations is governed by outer crossings that are independent of input channel. Values for  $H^-$  impact cross sections indicate qualitative behavior similar to that for H impact, but the outer electron clearly must be taken into account.

\*Present address: 6519 4th N.E., Seattle, Wash. 98115.

†Supported in part by the National Science Foundation.

‡Present address: Department of Physics, North Carolina State University, Raleigh, N.C. 27607.

<sup>1</sup>A. L. Orbeli, E. P. Andreev, V. A. Ankudinov, and V. M. Dukel'skii, *Zh. Eksp. Teor. Fiz.* **58**, 1938 (1970) [*Sov. Phys. JETP* **31**, 1044 (1970)].

<sup>2</sup>(a) J. S. Risley, C. B. Kerkdijk, and F. J. deHeer (unpublished); (b) J. S. Risley, F. J. deHeer, and C. B. Kerkdijk, in *Abstracts of Papers of the Ninth International Conference on the Physics of Electronic and Atomic Collisions*, edited by J. S. Risley and R. Geballe (Univ. of Washington Press, Seattle, 1975), p. 33.

<sup>3</sup>W. Wien, *Ann. Phys. (Leipz.)* **30**, 369 (1909).

<sup>4</sup>L. Kay, *Phys. Lett.* **5**, 36 (1962); for a recent compendium of beam-foil results see *Proceedings of the Third International Conference on Beam Foil Spectroscopy*, in *Nucl. Instrum. and Meth.* Vol. **110** (edited by S. Bashkin).

<sup>5</sup>R. H. Hughes, H. R. Dawson, B. M. Doughty, D. B. Kay, and C. A. Stigers, *Phys. Rev.* **146**, 53 (1966).

<sup>6</sup>S. K. Allison, *Rev. Mod. Phys.* **30**, 1137 (1958).

<sup>7</sup>H. A. Bethe and E. E. Salpeter, in *Encyclopedia of Physics*, Vol. XXXV, *Atoms I* (Springer-Verlag, Berlin, 1957), Sec. 67, p. 370.

<sup>8</sup>H. R. Dawson and D. H. Loyd, *Phys. Rev. A* **9**, 166

- (1974).
- <sup>9</sup>U. Fano and J. H. Macek, *Rev. Mod. Phys.* 45, 553 (1973).
- <sup>10</sup>R. H. Hughes and H. Kisner, *Phys. Rev. A* 5, 2107 (1972); R. V. Krotkov, F. W. Byron, Jr., J. A. Medeiros, and K. H. Yang, *Phys. Rev. A* 5, 2078 (1972); V. Dose, R. E. Olson, P. Pradel, F. Roussel, A. S. Schlachter, and G. Speiss, *Phys. Rev. A* 12, 1261 (1975).
- <sup>11</sup>R. H. Hughes, R. C. Waring, and C. Y. Fan, *Phys. Rev.* 122, 525 (1961).
- <sup>12</sup>M. Harnois, J. S. Risley, and R. Geballe, in *Ref. 2(b)*, p. 35.
- <sup>13</sup>M. Harnois, Ph.D. dissertation (Univ. of Washington, Seattle) (unpublished), available from University Microfilms, Ann Arbor, Mich.
- <sup>14</sup>A. L. Orbeli, E. P. Andreev, V. A. Ankudinov, and V. M. Dukel'skii, *Zh. Eksp. Teor. Fiz.* 57, 108 (1959) [*Sov. Phys. JETP* 30, 63 (1969)]; R. H. Hughes, H. M. Petefish, and H. Kisner, *Phys. Rev. A* 5, 2103 (1972); E. P. Andreev, V. A. Ankudinov, and S. V. Bobashev, *Zh. Eksp. Teor. Fiz.* 50, 565 (1966) [*Sov. Phys. JETP* 23, 375 (1966)]; R. H. Hughes, C. A. Stigers, B. M. Doughty, and E. D. Stokes, *Phys. Rev. A* 1, 1424 (1970); R. H. Hughes, H. R. Dawson, and B. M. Doughty, *Phys. Rev.* 164, 166 (1967).
- <sup>15</sup>J. H. Birely and R. J. McNeal, *Phys. Rev. A* 5, 257 (1972).
- <sup>16</sup>G. F. Drukarev, *Zh. Eksp. Teor. Fiz.* 58, 2210 (1970) [*Sov. Phys. JETP* 31, 1193 (1970)].
- <sup>17</sup>J. S. Risley and R. Geballe, *Phys. Rev. A* 9, 2485 (1974).
- <sup>18</sup>W. Lichten, *Phys. Rev.* 164, 131 (1967); M. Barat and W. Lichten, *Phys. Rev. A* 6, 211 (1972).